Hyperactivity of Anterior Cingulate Cortex Areas 24a/24b Drives Chronic Pain-Induced Anxiodepressive-like Consequences

Jim Sellmeijer, Victor Mathis, Sylvain Hugel, Xu-Hui Li, Qian Song, Qi-Yu Chen, Florent Barthas, Pierre-Eric Lutz, Meltem Karatas, Andreas Lüthi, et al.

Neurobiology of Disease

Hyperactivity of Anterior Cingulate Cortex Areas 24a/24b Drives Chronic Pain-Induced Anxiodepressive-like Consequences

Jim Sellmeijer,[1,2,3] Victor Mathis,[1] Sylvain Hugel,[1] Xu-Hui Li,[5] Qian Song,[5] Qi-Yu Chen,[5] Florent Barthas,[1] Pierre-Eric Lutz,[1] Meltem Karatas,[1] Andreas Luthi,[2] Pierre Veinante,[1] Ad Aertsen,[3] Michel Barrot,[1] Min Zhuo,[4,5] and Ipek Yalcin[1]

[1]Centre National de la Recherche Scientifique, Université de Strasbourg, Institut des Neurosciences Cellulaires et Intégratives, 67000 Strasbourg, France, [2]Friedrich Miescher Institute for Biomedical Research, 4058 Basel, Switzerland, [3]Faculty of Biology and Bernstein Center Freiburg, University of Freiburg, D-79104 Freiburg, Germany, [4]Department of Physiology, Faculty of Medicine, University of Toronto, Toronto, Ontario M5S 1A8, Canada, and [5]Center for Neuron and Brain Disease, Frontier Institutes of Science and Technology, Xi'an Jiaotong University, Xi'an, 710049, China

Pain associates both sensory and emotional aversive components, and often leads to anxiety and depression when it becomes chronic. Here, we characterized, in a mouse model, the long-term development of these sensory and aversive components as well as anxiodepressive-like consequences of neuropathic pain and determined their electrophysiological impact on the anterior cingulate cortex (ACC, cortical areas 24a/24b). We show that these symptoms of neuropathic pain evolve and recover in different time courses following nerve injury in male mice. *In vivo* electrophysiological recordings evidence an increased firing rate and bursting activity within the ACC when anxiodepressive-like consequences developed, and this hyperactivity persists beyond the period of mechanical hypersensitivity. Whole-cell patch-clamp recordings also support ACC hyperactivity, as shown by increased excitatory postsynaptic transmission and contribution of NMDA receptors. Optogenetic inhibition of the ACC hyperactivity was sufficient to alleviate the aversive and anxiodepressive-like consequences of neuropathic pain, indicating that these consequences are underpinned by ACC hyperactivity.

Key words: **anterior cingulate cortex; anxiety; depression; electrophysiology; neuropathic pain; optogenetics**

Significance Statement

Chronic pain is frequently comorbid with mood disorders, such as anxiety and depression. It has been shown that it is possible to model this comorbidity in animal models by taking into consideration the time factor. In this study, we aimed at determining the dynamic of different components and consequences of chronic pain, and correlated them with electrophysiological alterations. By combining electrophysiological, optogenetic, and behavioral analyses in a mouse model of neuropathic pain, we show that the mechanical hypersensitivity, ongoing pain, anxiodepressive consequences, and their recoveries do not necessarily exhibit temporal synchrony during chronic pain processing, and that the hyperactivity of the anterior cingulate cortex is essential for driving the emotional impact of neuropathic pain.

Introduction

Mood disorders, such as anxiety and depression, are frequently observed in patients suffering from chronic pain, which adds dramatically to the patients' pain burden (Radat et al., 2013). Preclinical studies have shown that the anxiodepressive-like consequences of chronic pain, as in neuropathic pain condition, can be studied in murine models (Narita et al., 2006; Yalcin et al., 2011; Alba-Delgado et al., 2013) and further highlight the im-

Received Nov. 7, 2017; revised Jan. 10, 2018; accepted Feb. 10, 2018.

Author contributions: A.L., A.A., M.B., M.Z., and I.Y. designed research; J.S., V.M., S.H., X.-H.L., Q.S., Q.-Y.C., F.B., M.K., and I.Y. performed research; J.S., S.H., X.-H.L., Q.S., Q.-Y.C., F.B., P.-E.L., P.V., A.A., M.Z., and I.Y. analyzed data; J.S. and I.Y. wrote the paper.

This work was supported by the Centre National de la Recherche Scientifique Contract UPR3212, the University of Strasbourg, the NeuroTime Erasmus Mundus Joint doctorate, and Brain & Behavior Research Foundation National Alliance for Research on Schizophrenia and Depression Young Investigator Grant 18893 to I.Y. P.-E.L. was supported by Fondation pour la Recherche Médicale and Fondation Deniker fellowships. M.Z. was supported by Canada Research Chair, Canadian Institutes of Health Research Operating Grant MOP-124807, and Azrieli Neurodevelopmental Research Program and Brain Canada. We thank Stéphane Doridot for assistance in breeding mice and in genotyping; Elaine Gravel for technical support; and Dr. Modesto R. Peralta for English editing.

The authors declare no competing financial interests.

Correspondence should be addressed to Dr. Ipek Yalcin, Centre National de la Recherche Scientifique, Université de Strasbourg, Institut des Neurosciences Cellulaires et Intégratives, 67000 Strasbourg. E-mail: yalcin@inci-cnrs.unistra.fr.

DOI:10.1523/JNEUROSCI.3195-17.2018

 0270-6474/18/383102-14$15.00/0

portance of the time factor in the development of these consequences (Yalcin et al., 2011; Barthas et al., 2015). It has been recently shown that depressive-like behaviors are still present 2 weeks after recovery from mechanical hypersensitivity in an animal model of neuropathic pain (Dimitrov et al., 2014), raising the question of whether these consequences of chronic pain might be maintained in the long-term independently from sensory aspects.

The anterior cingulate cortex (ACC) is involved in the processing of both pain and mood-related information (Shackman et al., 2011; Bliss et al., 2016). The implication of the ACC in depression is supported by a hyperactivity of the ACC in depressed patients (Mayberg et al., 1999; Drevets et al., 2002; Yoshimura et al., 2010), and by changes in the mouse ACC transcriptome that are correlated with depressive-like behaviors in the chronic stress model (Surget et al., 2009). Clinical imaging studies also show the recruitment of the ACC in pain processing (Peyron et al., 2000), and preclinical studies more precisely associate the activation of ACC neurons with pain-like aversive (Johansen et al., 2001; Barthas et al., 2015) or fearful (Tang et al., 2005) behaviors. Potentiation of synaptic responses (Xu et al., 2008; Chen et al., 2014), disinhibition (Blom et al., 2014), and increased excitability (Li et al., 2010; Cordeiro Matos et al., 2015) are also observed *ex vivo* in the ACC in rodent models of chronic pain. *In vivo* studies further show that a lesion of the ACC prevents both chronic pain-induced anxiodepressive-like behaviors (Barthas et al., 2015) and the aversiveness of ongoing pain (Johansen et al., 2001; King et al., 2009; Qu et al., 2011; Barthas et al., 2015). In addition, it has been reported that (1) optogenetic activation of pyramidal neurons within the ACC is sufficient to induce anxiodepressive-like behaviors in naive mice (Barthas et al., 2015) and that (2) these behaviors are associated with transcriptomic changes in the ACC (Barthas et al., 2017). Finally, presynaptic LTP in the ACC has been linked to pain-related anxiety (Koga et al., 2015).

Accordingly, the ACC seems to be a critical brain region implicated in different symptoms of chronic pain, and especially in its anxiodepressive-like consequences (Barthas et al., 2015; Koga et al., 2015).

In the present study, we first aimed at characterizing the long-term evolution, over 6 months, of mechanical hypersensivity, of the aversive state induced by ongoing pain, and of the anxiodepressive-like consequences of neuropathic pain in mice using the "cuff" model. This model, based on sciatic nerve cuffing, has the advantage of displaying spontaneous recovery from mechanical allodynia (Yalcin et al., 2014b), which allows studying the behavioral consequences of neuropathic pain in the presence and absence of hypersensitivity. We also determined the time course of *in vivo* electrophysiological alterations accompanying these various symptoms within the ACC (cortical areas 24a/24b) (Fillinger et al., 2017b), and correlated them to the different stages of the pathology.

This long-term characterization evidenced that the mechanical hypersensitivity, aversiveness of ongoing pain, and anxiety/depressive-like consequences of neuropathic pain evolve in distinct time courses. The *in vivo* electrophysiological recordings further showed a correlation between ACC hyperactivity and the aversive and anxiodepressive-like consequences. These results are reinforced by whole-cell patch-clamp recordings highlighting a facilitation of excitatory synaptic transmission onto ACC pyramidal neurons in cuff-implanted animals showing depressive-like consequences. Moreover, we showed that optogenetic inhibition of the ACC was sufficient to counteract the chronic pain-induced emotional consequences, which supports a causal link between ACC hyperactivity and the emotional aspects of neuropathic pain.

Materials and Methods

Animals

Experiments were conducted using male adult C57BL/6J (RRID:IMSR_JAX:000664) mice (Charles River), group-housed with a maximum of 5 animals per cage and kept under a reversed 12 h light/dark cycle. Only the animals used for optogenetic experiments were single housed after the optic fiber implantation to avoid possible damage to the implant. Behavioral tests were conducted during the dark phase under red light. The Chronobiotron animal facilities are registered for animal experimentation (Agreement A67-2018-38), and protocols were approved by the local ethical committee of the University of Strasbourg (CREMEAS, #02015021314412082).

Surgical procedures

Surgical procedures were performed under ketamine/xylazine anesthesia (ketamine 17 mg/ml, xylazine 2.5 mg/ml; i.p., 4 ml/kg) (Centravet).

Neuropathic pain model. Neuropathic pain was induced by implanting a 2 mm section of PE-20 polyethylene tubing (Harvard Apparatus) around the main branch of the right sciatic nerve (Benbouzid et al., 2008; Barrot, 2012; Yalcin et al., 2014b). Before surgery, animals were assigned to experimental groups according to their initial mechanical nociceptive threshold, to even out the average mechanical threshold among groups. Animals in the sham condition underwent the same procedure without cuff implantation.

Virus injection. After anesthesia, C57BL/6J mice were placed in a stereotaxic frame (Kopf). The 0.5 μl of AAV5-CaMKIIa-eArchT3.0-EYFP (UNC Vector core) was injected bilaterally in the ACC (areas 24a/24b) using a 5 μl Hamilton syringe (0.05 μl/min, coordinates for the ACC: 0.7 mm from bregma, lateral: $\pm$0.3 mm, dorsoventral: $-$1.5 mm from the skull). After injection, the 32 gauge needle remained in place for 10 min and then the skin was sutured.

Optic fiber cannula implantation. Four weeks after virus injection, the animals underwent optic fiber cannula implantation. The mice were implanted unilaterally over the site of virus injection. Cannulas were implanted in the left hemisphere in half of each experimental group, whereas the other half received the implant in the right hemisphere. The optic fiber cannula was 1.7 mm long and 220 μm in diameter. The cannula was inserted 1.5 mm deep in the brain (MFC_220/250–0.66_1.7mm_RM3_FLT, Doric Lenses) (Barthas et al., 2015).

Optogenetic procedures

After a 3 to 7 d recovery period, we performed behavioral experiments. Green laser light (custom assembly, Green 520 nm, 16 mW, Miniature Fiber Coupled Laser Diode Module, Doric Lenses) was delivered through a 0.75-m-long monofiber optic patch chord (MFP_240/250/2000–0.63_0.75m_FC-CM3, Doric Lenses) that was mounted to the optic fiber implant on the skull. Optogenetic inhibition was performed either before or during behavioral testing, by continuous light for 5 min with a power of 16 mW. Control animals underwent the same procedures but the light was turned off during stimulation protocols.

Behavioral analysis

Behavioral testing was performed during the dark phase, under red light. While each mouse went through different tests, those were conducted according to the following rules: excepted for the von Frey results, no mouse went twice through the same test (i.e., the different time points (TPs) for a given test were performed on independent sets of animals); the forced swim test was always considered as terminal (i.e., no other test was done on mice after they went through forced swimming). Each graph displayed in Figure 2 is from a given (single) batch of animals, with Sham and Cuff mice from this batch tested on the same day(s) to always ensure internal control, and with von Frey data always available the same week for these mice. Thus, for this general characterization, we did not mix results from different batches within a given graph of Figure 2, and we always had the hypersensitivity status of the animals to justify the hyper-

sensitivity component of the TP clustering. Mechanical threshold and anxiodepressive-like behaviors of animals used for electrophysiology studies were determined before recordings.

Nociceptive testing. von Frey filaments were used to determine the mechanical threshold of hindpaw withdrawal (Bioseb). Mice were placed in Plexiglas boxes (7 cm × 9 cm × 7 cm) on an elevated mesh screen. After 15 min habituation, animals were tested by applying a series of ascending forces (0.16–8 g) on the plantar surface of each hindpaw. Each filament was tested 5 times per paw, applied until it just bent (Yalcin et al., 2014b; Barthas et al., 2015). The threshold was defined as 3 or more withdrawals observed out of the 5 trials. To characterize changes in mechanical thresholds during an extended period, we tested animals before and at given TPs after sciatic nerve surgery. The animals used for optogenetic inhibition of the ACC were tested before sciatic nerve surgery and before the behavioral tests. Finally, we tested the animals during light stimulation to see whether optogenetic inhibition affected mechanical thresholds.

Conditioned place preference (CPP). To test the motivational drives resulting from the aversive state induced by ongoing pain and from its relief by clonidine, a single-trial CPP paradigm was used (King et al., 2009). In this test, animals develop a preference to a clonidine-paired chamber due to both pain relief in this environment and avoidance for the saline-paired chamber associated with ongoing pain. The apparatus consisted of 3 Plexiglas chambers separated by manually operated doors (Imetronic). Two chambers (15 cm × 24 cm × 33 cm), distinguished by the texture of the floor and by the wall patterns, were connected by a central chamber (15 cm × 11 cm × 33 cm). Animals went through a 3 d preconditioning period during which they had access to all chambers for 30 min each day. Time spent in each chamber was analyzed to control for the lack of preference for one of the chambers. Animals spending >75% or <25% of the total time in one of the chambers were excluded from the study. On the conditioning day (day 4), mice first received intrathecal saline (10 μl) and were placed in a conditioning chamber. Four hours later, mice received clonidine (10 μg/10 μl), an α2-adrenoceptor agonist inducing analgesia after intrathecal administration, and were placed in the opposite chamber. Conditioning lasted 15 min per chamber, without allowing the animal to access the other chambers. On the fifth day, mice were placed in the center chamber, with free access to both conditioning chambers, and the time spent in each chamber was recorded for 30 min. CPP was assessed in separate sets of mice corresponding to 8 weeks (TP2), 14 weeks (TP3), and 22 weeks (TP4) after cuff implantation. The exact TP status of the animals was each time determined using the von Frey test for mechanical hypersensitivity and by using the novelty suppressed feeding test for the anxiodepressive-like state.

To study whether optogenetic inhibition of the ACC caused a preference, we used another version of the CPP test, with a custom-made box with 2 chambers (23 cm × 22 cm × 16 cm), distinguishable by different wall patterns, and connected to each other by a single sliding door. The test lasted 4 d. On the first day, animals were habituated to the testing box by allowing them full access to both compartments for 5 min. During the second and third days, animals went through a conditioning period. For this purpose, during the mornings, the animals were placed in the compartment where they received no-light stimulation, whereas during the afternoon sessions the animals were light-stimulated following the above-mentioned protocol. Control animals underwent the same procedures, but during the afternoon session the laser light remained off. On the fourth day, we placed the animal at the level of the sliding door and measured the time spent in each compartment during 5 min.

Dark-light test. To measure anxiety-like behavior, we performed the dark-light test (Vogt et al., 2016), with a two compartment testing box (18 cm × 18 cm × 14.5 cm) connected by a dark tunnel (8.5 cm × 7 cm × 6 cm). One compartment was brightly illuminated (1500 lux), whereas the other was dark. Mice were placed in the dark compartment at the beginning of the test, and the time spent in the lit compartment was recorded for 5 min. This test was performed 2, 8, 11, and 15 weeks after sciatic nerve surgery in different sets of animals.

Novelty suppressed feeding (NSF) test. The NSF test was used to assess anxiodepressive-like behavior as it induces a conflict between the drive to eat and the fear of venturing into the center of the box (Yalcin et al., 2011; Barthas et al., 2015, 2017). For this test, we used a plastic box with the floor covered with 2 cm of sawdust. Animals were food deprived for 24 h. At the time of testing, a single pellet of food was placed in the middle of the testing chamber under 7 lux, and the latency to eat the pellet was recorded within a 5 min period. The NSF test was performed 2, 8, 11, 16, 18, and 21 weeks after sciatic nerve surgery in independent sets of animals. For the optogenetic experiment, the NSF test was performed immediately after the inhibition procedure.

Splash test. This test was used to measure grooming behavior indirectly (Yalcin et al., 2011; Barthas et al., 2015) because decreased grooming can be related to the loss of interest in performing self-relevant tasks. This behavior was measured for 5 min after spraying a 10% sucrose solution on the coat of the animals. The splash test was performed on animals 3, 9, 12, 14, and 16 weeks after the peripheral nerve injury in independent sets of animals. For the optogenetic experiment, the splash test was performed during the inhibition procedure.

Forced swimming test. This test was performed to evaluate despair-like behavior (Porsolt et al., 1977). We lowered the mouse into a glass cylinder (height 17.5 cm, diameter 12.5 cm) containing 11.5 cm of water (23°C–25°C). The test duration was 6 min; but because only little immobility was observed during the first 2 min, we only quantified the duration of immobility during the last 4 min of the test. We considered the mouse to be immobile when it floated upright in the water, with only minor movements to keep its head above the water. This test was performed 7, 14, 17, 18, and 21 weeks after the sciatic nerve surgery in different sets of animals.

Locomotor activity. At three different TPs, locomotor activity was monitored in both sham and cuff-implanted mice. Mice were individually placed in activity cages with photocell beams. The number of beam breaks was recorded over 1 h.

Ex vivo *electrophysiological recordings*

We performed whole-cell patch-clamp recordings of neurons from the layer II/III of the ACC. Local electrical stimulation was delivered by a bipolar stimulation electrode placed in layer V/VI of the ACC. For these experiments, mice were killed by decapitation and the brain was removed, then immediately immersed in cold (0°C-4°C) sucrose-based ACSF containing the following (in mM): 2 kynurenic acid, 248 sucrose, 11 glucose, 26 $NaHCO_3$, 2 KCl, 1.25 KH_2PO_4, 2 $CaCl_2$, and 1.3 $MgSO_4$ (bubbled with 95% O_2 and 5% CO_2). Transverse slices (300 μm thick) were cut with a vibratome (VT1000S, Leica). Slices were maintained at room temperature in a chamber filled with ACSF containing the following (in mM): 126 NaCl, 26 $NaHCO_3$, 2.5 KCl, 1.25 NaH_2PO_4, 2 $CaCl_2$, 2 $MgCl_2$, and 10 glucose (bubbled with 95% O_2 and 5% CO_2; pH 7.3; 310 mOsm measured). Slices were transferred to a recording chamber and continuously superfused with ACSF saturated with 95% O_2 and 5% CO_2. Pyramidal ACC neurons were recorded in the whole-cell patch configuration. Patch pipettes were pulled from borosilicate glass capillaries (Harvard Apparatus) using a P-1000 puller (Sutter Instruments). For optogenetic experiments performed in AAV5-CaMKIIa-eArchT3.0-EYFP-injected animals, pipettes were filled with a solution containing the following (in mM): 145 KCl, 10 HEPES, and 2 $MgCl_2$. For mEPSCs recordings, pipettes were filled with a solution containing the following (in mM): 75 Cs_2SO_4, 10 CsCl, 10 HEPES, and 2 $MgCl_2$. The pH of intrapipette solutions was adjusted to 7.3 with KOH, and osmolarity to 310 mOsm with sucrose. With this solution, the patch pipettes had an open tip resistance from 3.5 to 4.5 MΩ. Recordings were performed in the presence of CNQX (10 μM) and bicuculline (10 μM) for optogenetic experiments, whereas mEPSCs were recorded with TTX (0.5 μM) in the recording solution. For optogenetic experiments, the ACC was illuminated with the same system used for the *in vivo* experiments (see below) triggered with WinWCP 4.3.5, the optic fiber being localized in the recording chamber at 3 mm from the recorded neuron. In voltage-clamp mode, the holding potential was fixed at −60 mV, and in current-clamp mode at a holding current allowing maintaining the resting neuron at ~−60 mV. Recordings were acquired with WinWCP 4.3.5 (courtesy of

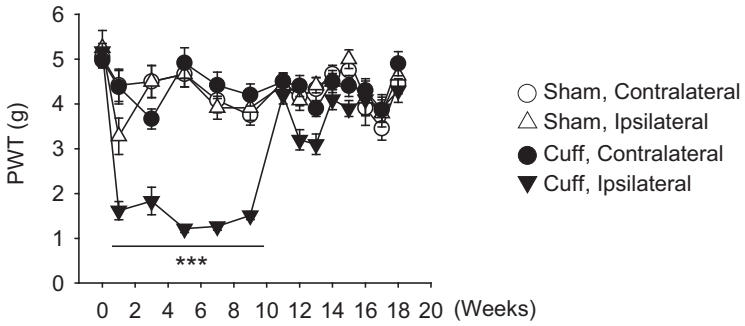

Figure 1. Nerve injury induces mechanical hypersensitivity. In C57BL/6J mice, unilateral sciatic nerve compression induces an ipsilateral long-lasting mechanical hypersensitivity which lasts ~11 weeks. After this period, mechanical thresholds return back to sham levels spontaneously. Sham, $n = 24$; Cuff, $n = 24$. Data are mean ± SEM. ***$p < 0.001$. PWT, Paw withdrawal threshold.

Dr. J. Dempster, University of Strathclyde, Glasgow, United Kingdom). All recordings were performed at 34°C.

In vivo *electrophysiological recordings*

Animals were anesthetized in an induction box with a 2% isoflurane/air mixture (Vetflurane, Virbac) and then placed in a Kopf stereotaxic frame (KOPF 1730) equipped with a tight nose mask to continuously deliver the anesthesia.

A 1 × 1.4 mm cranial window was prepared directly anterior to the bregma, ranging from −0.7 to 0.7 mm lateral from the midline. The dura was opened to lower the glass electrode into the brain. Recordings of spontaneous activity were performed using sharp electrodes pulled from borosilicate micropipettes (1.2 mm outer and 0.69 mm inner diameters, Harvard Apparatus, 30–0044), with a Narashige pipette puller (tip diameter < 1 μm, resistance ±25 MΩ). The glass electrodes were filled with 0.5 M potassium acetate solution. The signal from the electrode was recorded by a silver wire, amplified using an operational amplifier (Neurodata IR-183A, Cygnus Technology; gain × 10), and then amplified further and filtered using a differential amplifier (Model 440, Brownlee Precision; gain × 100; bandpass filter 0.1–10 kHz). The signal was then digitized with a CED digitizer (sampling rate: 20 kHz) and recorded with Spike2 software (version 7.12b, Cambridge Electronic Design). Raw data files were exported into MATLAB (The MathWorks) and analyzed with custom-made MATLAB scripts, which are available in a bitbucket repository entitled Sellmeijer, 2016.

During the recording procedure, isoflurane anesthesia was lowered to 0.5%–0.75% and was monitored by regular paw pinching. The glass pipette was slowly lowered using a Scientifica one-dimensional micromanipulator, and recordings were made between 0.2 and 1.0 mm anterior to the bregma ranging from −0.5 to 0.5 mm from the midline, which corresponds to layers II/III of the cortex. Neurons were recorded from the brain surface until 1500 μm deep. Once stable cell activity was detected, a 5 min segment of spontaneous activity was recorded. Recording sites were marked by iontophoretically injecting a 4% Pontamine Sky blue dye (Sigma-Aldrich) in 0.5 M sodium-acetate solution (Sigma-Aldrich). At the end of the recording, the mice were perfused, the brain was collected, and 40 μm sections were cut on a cryostat. The position of recorded cells was registered using the microdrive reference point with respect to the Pontamine Sky blue dye deposit.

Firing rate and bursting activity were calculated. Bursting activity, defined as ≥3 spikes within a 50 ms time window, was analyzed by calculating the total number of bursting events within a 90 s data segment. Neurons in which >20% of action potentials occurred in a bursting event were considered bursting neurons. The average number of spikes within a bursting event was also calculated.

Experimental design and statistical analysis

Before starting experiments, based on our previous behavioral studies, we estimated the sample size by using power analysis. All behavioral tests, *in vivo* electrophysiological recordings, and experiments using optogenetic approach were replicated several times. For each group, the mechanical sensitivity and anxiodepressive-like behaviors were analyzed before recordings and optogenetic manipulation. The number of animals per group is indicated in each behavioral graph; and both the number of recorded cells and of animals per group is indicated in each electrophysiology graph. Data are mean ± SEM. When data were not normally distributed, the Kruskal–Wallis test was performed followed by Mann–Whitney *U post hoc* tests to compare the means. When data were normally distributed, groups were compared with ANOVA multiple group comparisons followed by Duncan *post hoc* analysis, or with the Student's *t* test. For the von Frey results, we used a multifactorial ANOVA, considering paws (ipsilateral vs contralateral) and TPs as two levels of dependent data, and surgery (sham vs cuff) as independent groups. Significance level was set to $p < 0.05$. Statistical analyses were performed with MATLAB 2014a (The MathWorks) and Statistica version 7.1 (Statsoft).

Results

Long-term characterization of different symptoms of neuropathic pain

It has been previously shown that the anxiodepressive-like consequences of neuropathic pain evolve over time (Suzuki et al., 2007; Gonçalves et al., 2008; Yalcin et al., 2011). Indeed, whereas mechanical hypersensitivity is immediately present following nerve injury in the cuff model, mice develop anxiety-related behaviors 3–4 weeks later, while depression-related behaviors are observed after 6–8 weeks (Yalcin et al., 2011). On the longer term, cuff-implanted animals recover spontaneously from mechanical hypersensitivity (example from one batch of mice: $F_{(13,260)} = 5.54$, $p = 6.9 \times 10^{-9}$; cuff<sham: first $p = 2.7 \times 10^{-6}$; week 3, $p = 8.8 \times 10^{-7}$; week 5, $p = 1 \times 10^{-6}$; week 7, $p = 1.8 \times 10^{-6}$; week 9, $p = 1.5 \times 10^{-6}$; Fig. 1). Depending on the considered batch of animals, this recovery happened between the 11th and 14th weeks after operation. However, it is to be noted that all mice displayed mechanical hypersensitivity up to the 10th weeks after operation, and that no mice was hypersensitive at 15 weeks after operation. This recovery from mechanical hypersensitivity raises the question of whether the aversiveness of ongoing pain and/or the anxiodepressive-like consequences of chronic pain also disappear or remain present.

As reported previously (Yalcin et al., 2011), the nerve-injured animals did not show anxiodepressive-like behaviors yet at 2 weeks after operation (dark-light test, Fig. 2*A*; NSF test, Fig. 2*C*) or at 3 weeks after operation (splash test, Fig. 2*B*), even though mechanical hypersensitivity was already present (VF: $p = 0.01$, Fig. 2*A*; $p = 0.0001$, Fig. 2*B*; $p = 0.001$, Fig. 2*C*). In the dark-light test, nerve-injured animals displayed increased anxiety-like behavior at 8 weeks after operation, as shown by the reduced time spent in the lit compartment ($p = 6.17 \times 10^{-4}$; Fig. 2*A*). This behavior disappeared at 11 and 15 weeks after operation, coinciding with the recovery from mechanical hypersensitivity in the same animals (Fig. 1). In contrast, in the splash test, decreased grooming behavior was present at 9 weeks after operation ($p = 0.01$), but also at 12 weeks ($p = 0.003$) and 14 weeks after operation ($p = 0.0011$) (Fig. 2*B*) despite that mechanical hypersensitivity was no longer present in these sets of animals at these last 2 TPs. The deficit in grooming behavior, however, disappeared at 16 weeks after operation (Fig. 2*B*). Recovery was even more delayed in the NSF test, for which an increased latency to feed was present at 8 ($p = 3.3 \times 10^{-4}$), 11 ($p = 0.0437$), and 16 weeks after operation ($p = 0.0016$) (with no mechanical hypersensitivity at

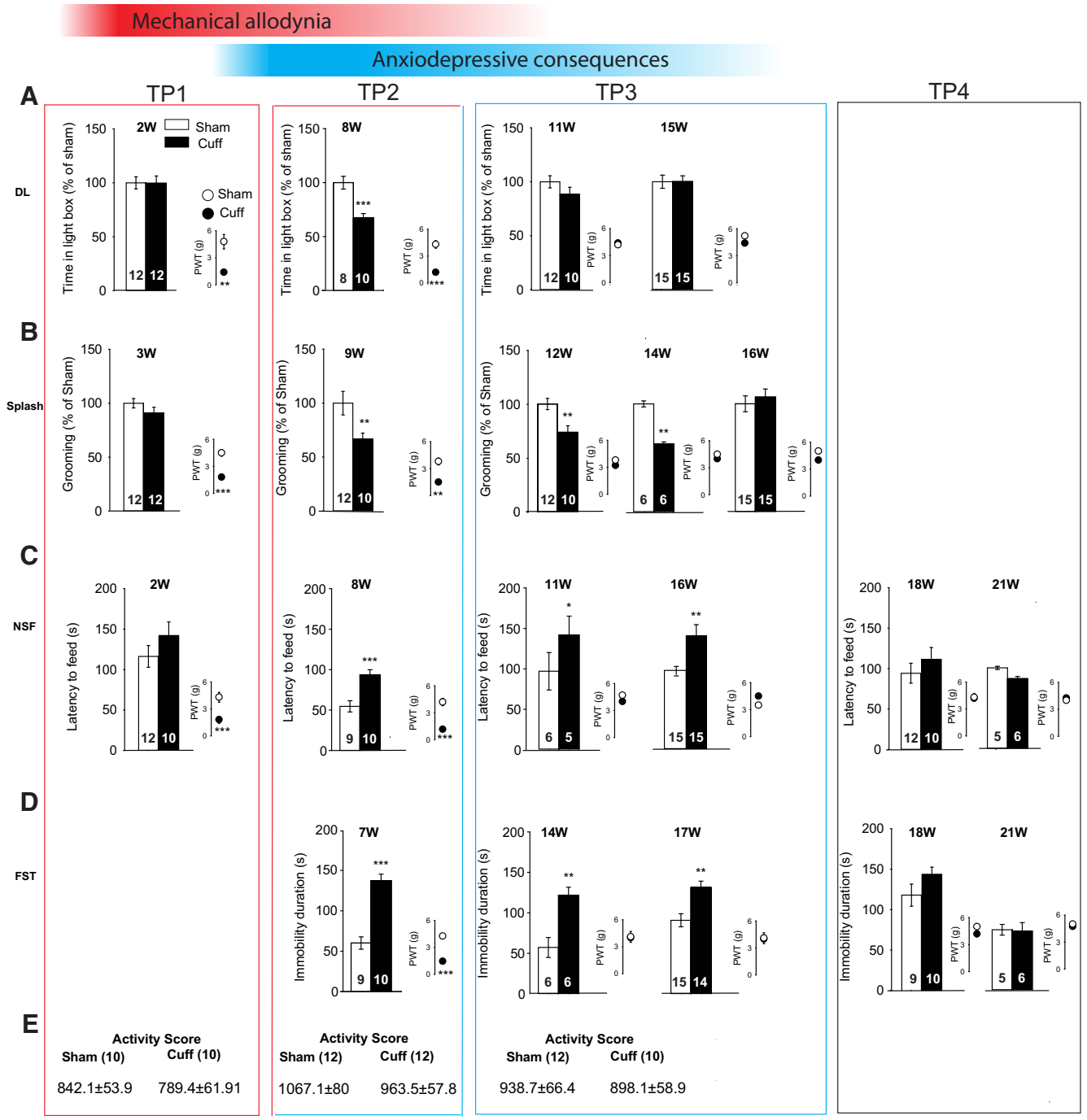

Figure 2. Long-term anxiodepressive-like consequences of neuropathic pain. Neuropathic pain induces anxiodepressive-like consequences, which disappear in a time-dependent manner. Sciatic nerve injury significantly: decreases the time spent in the lit compartment of the dark-light (DL) box at 8 but not at 2, 11, and 15 weeks (W) after operation (***A***), decreases grooming behavior in the splash test at 9, 12, and 14 but not at 3 and16 weeks after operation (***B***), increases the latency to feed in the NSF at 8, 11, 16 but not at 2, 18, 21 weeks after operation (***C***), increases immobility time at 7, 14, 17 but not at 18, 21 weeks after operation in the forced swimming test (FST) (***D***). Cuff-implanted animals did not show any locomotor activity deficits at TP1, TP2, and TP3 (***E***). For a given test, each TP was obtained in an independent set of mice and their corresponding von Frey results are presented nearby (***A–D***). TP1 corresponds to animals displaying mechanical hypersensitivity but not yet anxiodepressive-like consequences, TP2 corresponds to animals displaying both mechanical hypersensitivity and anxiodepressive-like consequences, TP3 corresponds to animals that recovered from mechanical hypersensitivity but still displayed depressive-like consequences, TP4 corresponds to animals that recovered from both mechanical hypersensitivity and anxiodepressive-like consequences. Data are mean ± SEM. Numbers in the bars or nearby activity scores indicate the number of animals. $*p < 0.05$, $**p < 0.01$, $***p < 0.001$. For other TP data between 2 weeks and 9 weeks after operation, see Yalcin et al. (2011).

these last 2 TPs), with recovery at 18 and 21 weeks after operation (Fig. 2*C*). The presence of depressive-like behavior as assessed using the forced swimming test was also long-lasting. Indeed, nerve-injured mice spent more time immobile at 7 ($p = 4.33 \times 10^{-5}$), 14 ($p = 0.0043$), and 17 weeks after operation ($p = 0.0023$) (with no mechanical hypersensitivity at these last 2 TPs) (Fig. 2*D*), and returned back to sham level only at 18 and 21 weeks after operation (Fig. 2*D*). Each von Frey result obtained the same week as the anxiodepressive behavioral tests is presented near the anxiodepressive behavioral graph (Fig. 2*A–D*).

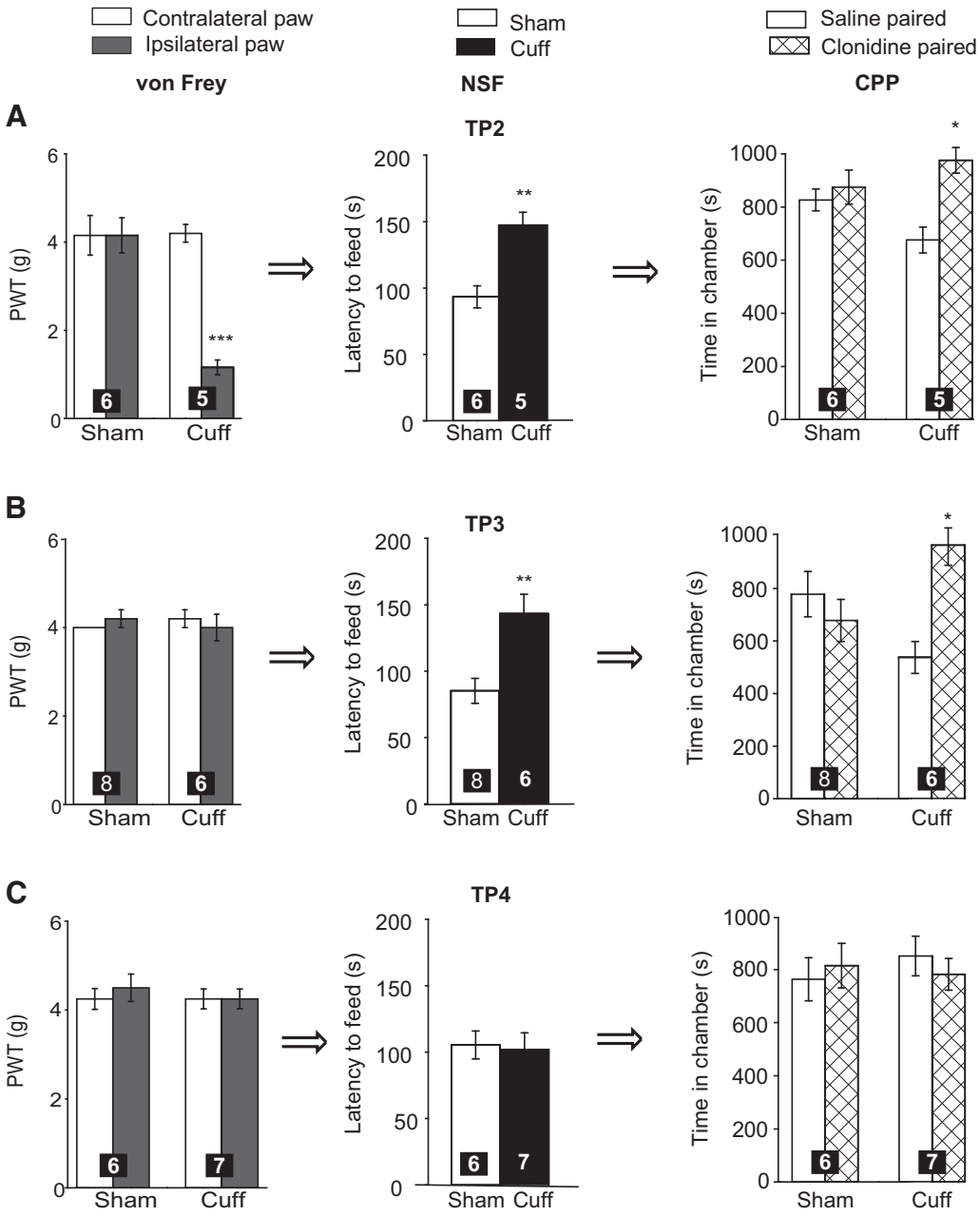

Figure 3. Nerve injury induces ongoing pain. ***A***, At TP2, animals displayed mechanical hypersensitivity, anxiodepressive-like behavior, and place preference for ongoing pain relief (10 μg clonidine, intrathecal). ***B***, At TP3, animals recovered from mechanical hypersensitivity but still displayed anxiodepressive-like consequences and place preference for ongoing pain relief. ***C***, At TP4, animals recovered from mechanical hypersensitivity and anxiodepressive-like behavior, and ongoing pain is no longer detected. Each TP corresponds to an independent experiment performed in separate sets of mice. Data are mean ± SEM. Numbers in the bars indicate the number of animals. *$p < 0.05$, **$p < 0.01$, ***$p < 0.001$. ** PWT, Paw withdrawal threshold.

Because the time course of recovery from mechanical hypersensitivity could slightly differ between batches of experiments, the results are presented according to 4 representative TPs for the rest of this study. TP1 corresponds to animals displaying mechanical hypersensitivity but not yet anxiodepressive-like consequences. TP2 corresponds to animals displaying both mechanical hypersensitivity and anxiodepressive-like consequences. TP3 corresponds to animals that recovered from mechanical hypersensitivity but still displayed depressive-like consequences. TP4 corresponds to animals that recovered from both mechanical hypersensitivity and anxiodepressive-like consequences.

As a control for behavioral tests, we checked the locomotor activity of animals over 1 h at different TPs and confirmed our previous reports (Barthas et al., 2015, 2017) by showing that locomotor activity was not significantly affected in cuff-implanted animals at the representative TP1, TP2, and TP3 (Fig. 2*E*).

We then tested the aversiveness of ongoing pain by using a CPP test. Clonidine was delivered intrathecally at lumbar level, which inhibits ascending inputs and leads to pain relief. Nerve-injured animals displayed a significant preference for the compartment associated with clonidine analgesia at TP2 ($F_{(1,9)} = 5.36$, $p = 0.04$; cuff saline vs cuff clonidine, $p = 0.017$; Figure 3*A*) but also at TP3 ($F_{(1,12)} = 5.219$, $p = 0.04$; cuff saline vs cuff clonidine, $p = 0.03$; Fig. 3*B*), despite the absence of mechanical hypersensitivity at this TP. Interestingly, this preference was no longer present at TP4 ($F_{(1,11)} = 0.36$, $p = 0.55$; Fig. 3*C*), suggesting a recovery from

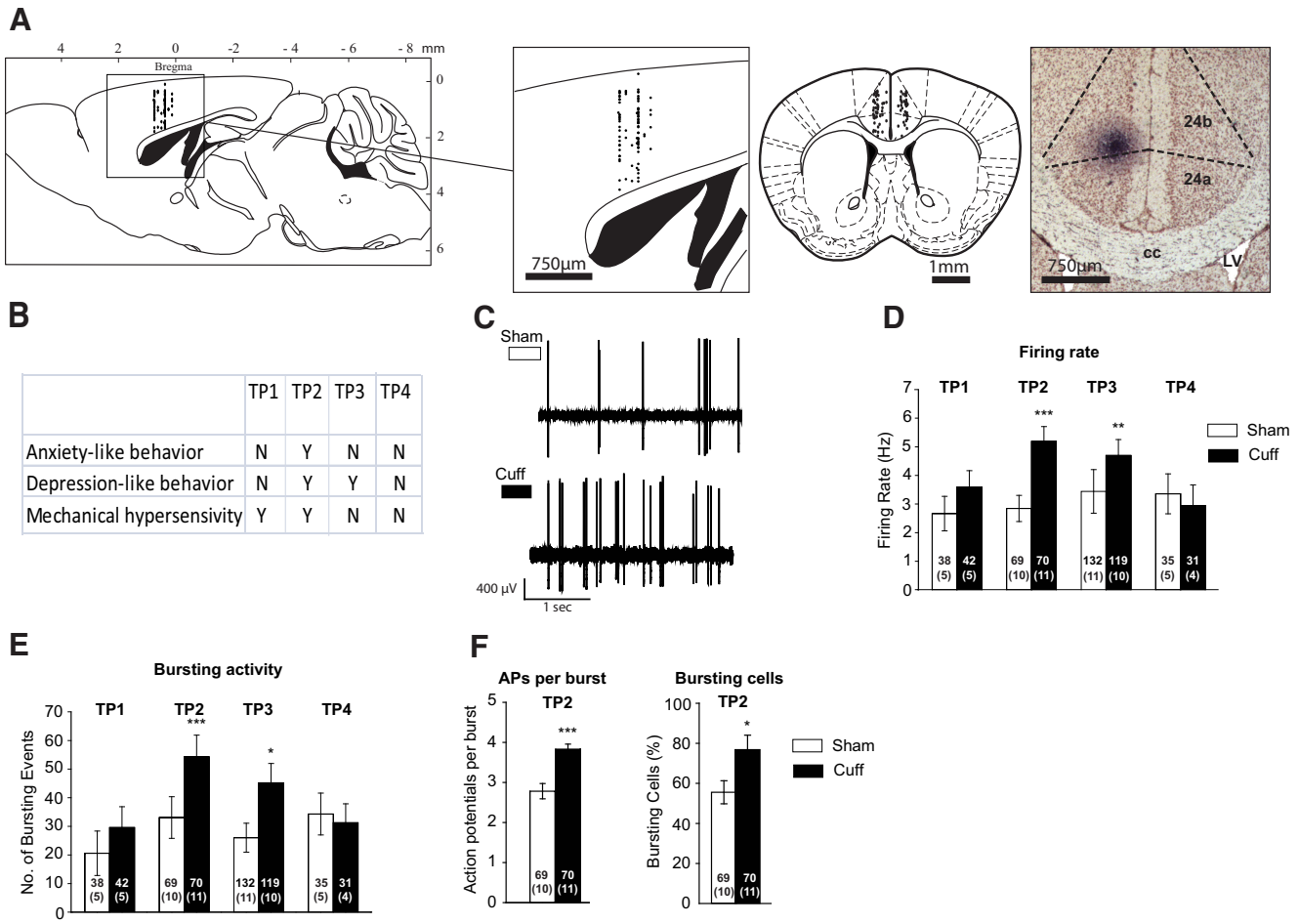

Figure 4. Increased ACC single-unit activity. ***A***, Illustration of the recording sites in the ACC (dots) on a sagittal and on a frontal plane. Right, Pontamine Sky blue dye deposit at the end of the recording. ***B***, Overview of the development and recovery of different aspects of neuropathic pain. Time frames of recorded animals correspond to 4 phenotypical TPs defined based on previous experiments (Fig. 2) and corresponding to the presence or absence of given behaviors. Each recorded animal was tested for mechanical hypersensitivity and anxiodepressive consequences. ***C***, Example of representative recordings from sham and nerve-injured animals at TP2. Single-unit firing rate (***D***) and bursting activity (***E***) are increased at TP2 and TP3 but not at TP1 and TP4. ***F***, Increased number of action potentials per burst and increased number of bursting cells at TP2. TP1 corresponds to animals displaying mechanical hypersensitivity but not yet anxiodepressive-like consequences. TP2 corresponds to animals displaying both mechanical hypersensitivity and anxiodepressive-like consequences. TP3 corresponds to animals that recovered from mechanical hypersensitivity but still displayed depressive-like consequences. TP4 corresponds to animals that recovered from both mechanical hypersensitivity and anxiodepressive-like consequences. Data are mean ± SEM. Numbers in the bars indicate the number of cells and animals. $*p < 0.05$, $**p < 0.01$, $***p < 0.001$. cc, Corpus callosum; LV, Lateral ventricle.

ongoing pain. See also Figure 3*A–C* for the state of mechanical hypersensitivity (TP2, $p = 6.2 \times 10^{-5}$; TP3, $p = 0.34$; TP 4, $p = 0.58$) and of anxiodepressive-like consequences (TP2, $p = 0.0028$; TP3, $p = 0.0014$; TP4, $p = 0.83$) in the same mice.

Together, these data show that ongoing pain and the depressive-like consequences of neuropathic pain can persist for weeks after the recovery from mechanical hypersensitivity.

ACC hyperactivity coincides with anxiodepressive-like consequences of neuropathic pain

To understand whether the spontaneous activity of the ACC is affected along the time-dependent evolution of neuropathic pain symptoms, we performed *in vivo* single-unit electrophysiological recording (Fig. 4*A*) at 4 different TPs (Fig. 4*B*). ACC neurons from nerve-injured animals had a significantly higher *in vivo* spontaneous firing rate at TP2 ($p = 3.52 \times 10^{-7}$) and TP3 ($p = 0.0022$; Fig. 4*C*,*D*), which was associated with an increase in bursting activity (TP2: $p = 5.50 \times 10^{-5}$, TP3: $p = 0.017$; Fig. 4*E*), in the number of action potentials per burst ($p = 3.42 \times 10^{-5}$, Fig. 4*F*) and in the number of bursting cells ($p = 0.034$; Fig. 4*F*) in nerve-injured animals at TP2. In the absence of anxiodepressive-like behaviors (i.e., at TP1, before affective symptoms developed; and at TP4, after affective symptoms recovered), the firing rate and bursting activity remained similar between sham and nerve-injured animals (Fig. 4*D*,*E*). No significant lateralization effect was measured for firing rate and bursting activity in cuff-implanted animals (data not shown).

Enhancement of excitatory synaptic transmission in the ACC coincides with anxiodepressive-like consequences of neuropathic pain

To assess the impact of neuropathic pain on synaptic transmission of pyramidal neurons, we recorded both paired-pulse ratio and miniature synaptic currents at TP2, when nerve-injured animals displayed depressive-like behavior. There was a significant reduction in the paired-pulse ratio of electrically evoked EPSCs, which provides support for presynaptic changes in nerve-injured mice ($F_{(1,120)} = 30.8$, $p < 0.001$; Fig. 5*A*). Both the amplitude and frequency of mEPSCs (amplitude: sham mice 7.8 ± 0.4 pA, cuff mice 9.8 ± 0.6 pA, $p < 0.05$; frequency: sham mice 1.2 ± 0.1 Hz, cuff mice 2.2 ± 0.2 Hz, $p < 0.01$; Fig. 5*B*) were significantly increased in nerve-injured mice, indicating that the facilitation of

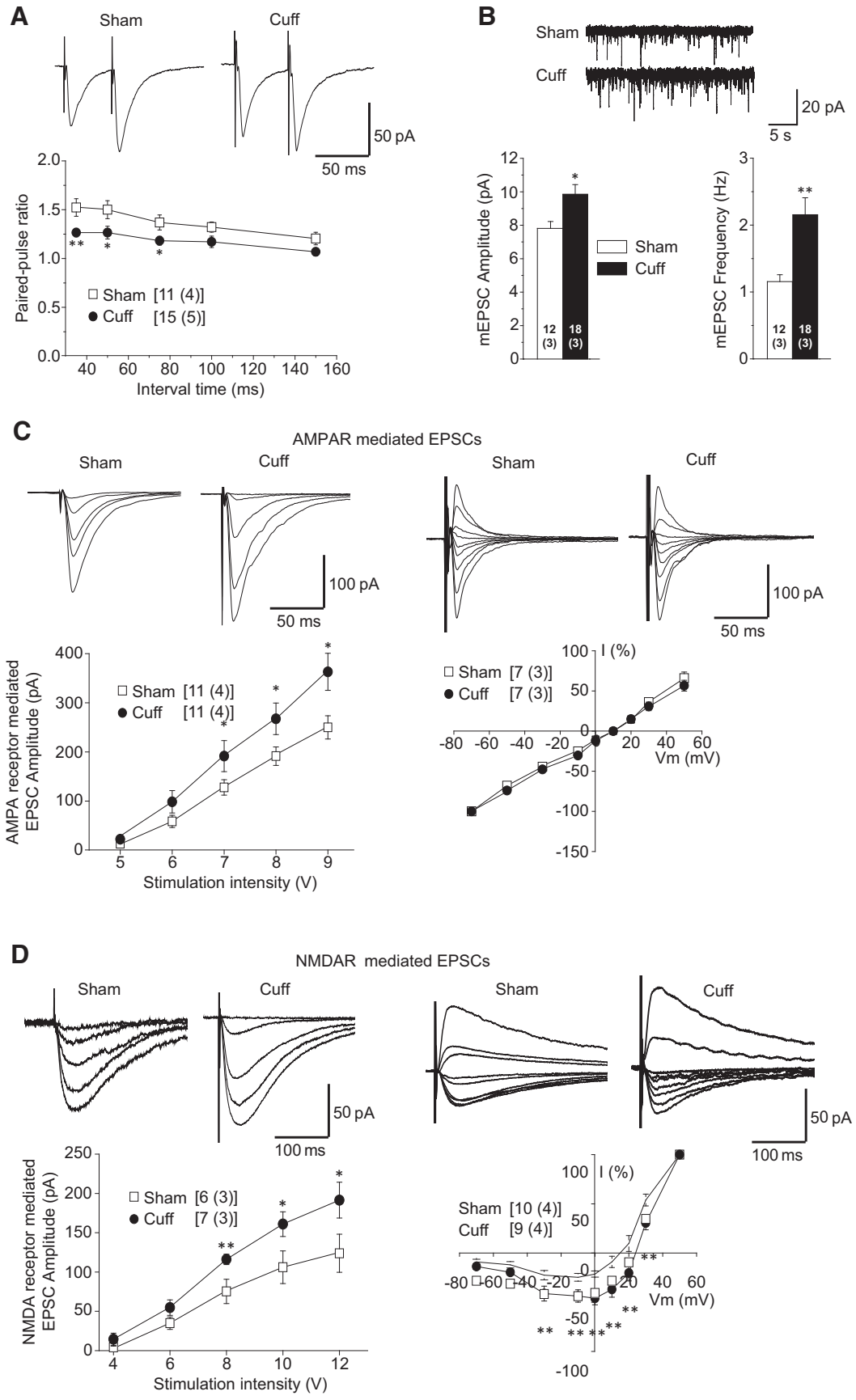

Figure 5. Facilitated presynaptic and postsynaptic ACC transmission in nerve-injured animals displaying depressive-like behaviors. ***A***, Samples (top) and summarized results (bottom) showed that the paired-pulse ratios, with recorded intervals of 35, 50, 75, 100, and 150 ms, were decreased in the cuff group compared with the sham group. ***B***, Samples (top) and summarized results (bottom) of the amplitude and frequency of mEPSCs. Both amplitude and frequency were increased in the cuff group compared with the sham group. (*Figure legend continues.*)

excitatory synaptic transmission onto pyramidal ACC neurons involved presynaptic and postsynaptic changes. Interestingly, both the slopes of the AMPAR-mediated input–output curve ($F_{(1,97)} = 17.1$, $p < 0.001$; Fig. 5*C*, left) and NMDAR-mediated input–output curve ($F_{(1,55)} = 7.7$, $p < 0.01$; Fig. 5*D*, left) were shifted to the left in nerve-injured mice, suggesting that an upregulation of AMPA and NMDA receptors could contribute to excitatory facilitation. We then tested the AMPAR and NMDAR-mediated *I–V* relationship and found that there was no difference in the AMPAR-mediated *I–V* between sham and nerve-injured mice ($F_{(1,108)} = 2.0$, $p = 0.15$; Fig. 5*C*, right). However, the NMDAR-mediated *I–V* curve differed between groups ($F_{(1,153)} = 61.3$, $p < 0.01$; Fig. 5*D*). When the same experiments were performed at TP3, which corresponds to animals still displaying depressive-like behaviors after recovery from mechanical hypersensitivity, we observed that the mEPSC frequency was still increased ($F_{(1,19)} = 8.974$; $p = 0.008$; Fig. 6), but not the paired-pulse ratio of evoked EPSCs. This finding indicates that the spontaneous release of glutamate was still enhanced in the ACC after the recovery from mechanical hypersensitivity. Neither the AMPAR nor the NMDAR-mediated input and output curves were altered. Interestingly, the NMDAR *I–V* curve remained different in the cuff group ($F_{(1,108)} = 15.54$; $p = 0.001$; Fig. 6).

Inhibition of the ACC relieves the emotional consequences of neuropathic pain

Based on our results demonstrating ACC hyperactivity in mice displaying anxiodepressive-like behaviors, we studied whether optogenetic inhibition of the ACC may counteract these consequences.

The delivery of AAV5-CaMKIIa-eArchT3.0-EYFP resulted in reliable virus transfection in the ACC, which was confirmed by EYFP fluorescence (Fig. 7*A*). To characterize the effect of green laser light illumination on transfected ACC neurons, we performed *ex vivo* electrophysiological recordings. Patch-clamp recordings showed that illumination with green light reliably inhibited spontaneous action potential firing in the current-clamp mode, and induced an outward current in the voltage-clamp mode (Fig. 7*B*).

In vivo, mechanical hypersensitivity was not affected by the ACC inhibition at either TP2 ($F_{(1,26)} = 60.29$, $p = 0.3 \times 10^{-8}$, cuff right < sham right, $p = 0.0001$) or TP3 ($F_{(1,20)} = 0.0032$, $p = 0.95$) (Fig. 7*C*). However, inhibition of the targeted ACC neurons induced a place preference in nerve-injured animals at both TPs (i.e., when mechanical hypersensitivity was still present) (TP2, $F_{(1,18)} = 5.42$, $p = 0.031$, cuff stimulated [light on] vs cuff control, $p = 0.006$) (Fig. 7*D*) or after it recovered (TP3, $F_{(1,8)} = 8.66$, $p = 0.018$, cuff stimulated [light on] vs cuff control, $p = 0.039$; Figure 7*D*), without having any effect in sham animals. These findings indicate that the inhibition of the CaMKIIa ACC neurons relieved the aversiveness of ongoing pain in nerve-injured mice.

Finally, we showed that optogenetic inhibition of the ACC also suppressed the anxiodepressive-like behaviors in nerve-injured animals, as observed by a normalization of grooming behavior in the splash test (Fig. 7*E*) at both TP2 ($p = 0.0033$, cuff no-light vs cuff light on) and TP3 ($p = 0.03$, cuff no-light vs cuff light on), and of the feeding latency in the NSF test at TP2 ($p = 0.0013$) (Fig. 7*F*). "No-light delivered" nerve-injured animals, however, still displayed characteristic chronic pain induced-behaviors (sham no-light vs cuff no-light grooming duration: $p = 0.03$, TP2; $p = 0.01$, TP3; Fig. 7*E*; sham no-light vs cuff no-light latency to feed: $p = 0.015$, TP2; $p = 0.015$, TP3; Fig. 7*F*). Together, our results show that a selective inhibition of ACC excitatory neurons is sufficient to alleviate the long-lasting consequences of neuropathic pain.

Discussion

We show here that different symptoms of neuropathic pain, including mechanical hypersensitivity, aversiveness of ongoing pain, and anxiodepressive-like consequences, display different time courses following nerve injury. The *in vivo* electrophysiological recordings showed an ACC hyperactivity coinciding with the time window of pain aversiveness and of anxiodepressive-like behaviors. *Ex vivo* patch-clamp recordings further supported ACC hyperactivity, as shown by increased excitatory postsynaptic transmission and increased contribution of NMDA receptors. Finally, our results show that optogenetic inhibition of the ACC can alleviate the aversiveness and anxiodepressive-like consequences of neuropathic pain.

A growing number of preclinical studies shows that the anxiodepressive-like consequences of chronic pain evolve over time (Yalcin et al., 2011; Alba-Delgado et al., 2013), raising the question of whether the various symptoms of neuropathic pain are interdependent or whether they develop separately. With the model and species used in this study, animals develop mechanical hypersensitivity immediately after nerve injury and spontaneously recover ~3 months later, which allows studying the behavioral consequences of neuropathic pain in the presence and absence of mechanical hypersensitivity. Patients with chronic pain also experience ongoing pain, which is rarely evaluated in preclinical studies. In animals, this symptom can be unmasked by alleviating the pain-related tonic aversive state in a CPP procedure (King et al., 2009; Barthas et al., 2015). For instance, lidocaine injected into the rostral ventromedial medulla, the brain area mediating descending modulation of pain (Wang et al., 2013), or spinal injection of clonidine (King et al., 2009; Barthas et al., 2015), induces place preference only in nerve-injured animals. In the present study, we also detected the presence of ongoing pain at TP3 (i.e., when mechanical hypersensitivity is no longer present), a finding that represents, to our knowledge, the first evidence in an animal model for a naturally occurring temporal dichotomy between evoked and ongoing pain. The hypersensitivity and ongoing pain that follow nerve injury have been proposed to share some mechanistic features. Indeed, both may imply an upregulation of voltage-gated Nav1.8 channels in primary afferent neurons (Yang et al., 2014), an alteration of descending pathways (Wang et al., 2013). and of spinal NK-1-positive ascending projections (King et al., 2011). Studies also pointed out that they can be distinguished mechanistically as well as neuroanatomically. An ACC lesion can block the aversiveness of ongoing pain in both neuropathic (Qu et al., 2011; Barthas et al., 2015) and inflammatory pain models without affecting mechanical hypersensitivity (Johansen et al., 2001; Chen et al., 2014; Barthas et al., 2015), whereas lesioning the posterior insular cortex can suppress the maintenance of mechanical hypersensitivity

←

(*Figure legend continued.*) ***C***, Samples (top) and summarized results (bottom) showed that the input–output curve of AMPARs-mediated EPSCs was steeper in the cuff group. However, the *I–V* curves were not changed. ***D***, Samples (top) and summarized results (bottom) showed that the input–output curve of NMDARs-mediated EPSCs was steeper in the cuff group. The *I–V* curve in the cuff group differed from that of the sham group. All experiments were performed at TP2 (8–9 weeks after surgery), which corresponds to animals displaying both mechanical hypersensitivity and anxiodepressive-like consequences. $^*p < 0.05$, $^{**}p < 0.01$. Numbers in bars or near group names indicate the numbers of cells and animals.

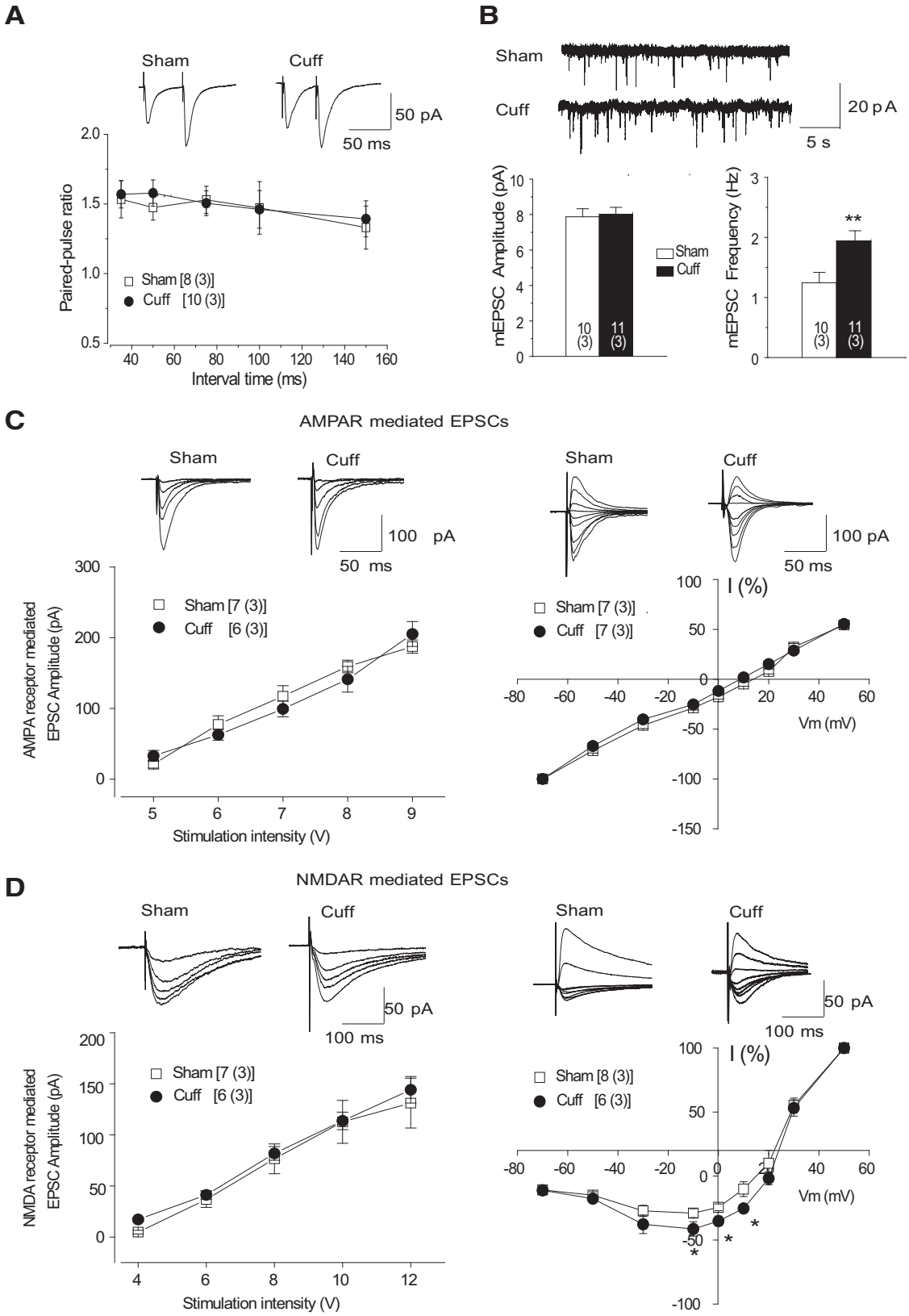

Figure 6. Facilitated presynaptic but nonpostsynaptic ACC transmission in nerve-injured animals, which recovered from mechanical hypersensitivity. ***A***, Samples (top) and summarized results (bottom) showed that the paired-pulse ratios, with recorded intervals of 35, 50, 75, 100, and 150 ms, were not changed in the cuff group compared with the sham group. ***B***, Samples (top) and summarized results (bottom) of the amplitude and frequency of mEPSCs. Frequency was increased in cuff group compared with the sham group. ***C***, Samples (top) and summarized results (bottom) showed that the input– output and *I–V* curves of AMPAR-mediated EPSCs were not changed in the cuff group. ***D***, Samples (top) and summarized results (bottom) showed that the input– output curve of NMDAR-mediated EPSCs was not different in the cuff group. The *I–V* curve in the cuff group differed from that of the sham group. All experiments were performed at TP3 (14–16 weeks after surgery), which corresponds to animals that recovered from mechanical hypersensitivity but still displayed depressive-like consequences. *$p < 0.05$, **$p < 0.01$. ** Numbers in bars or near group names indicate the number of cells and animals.

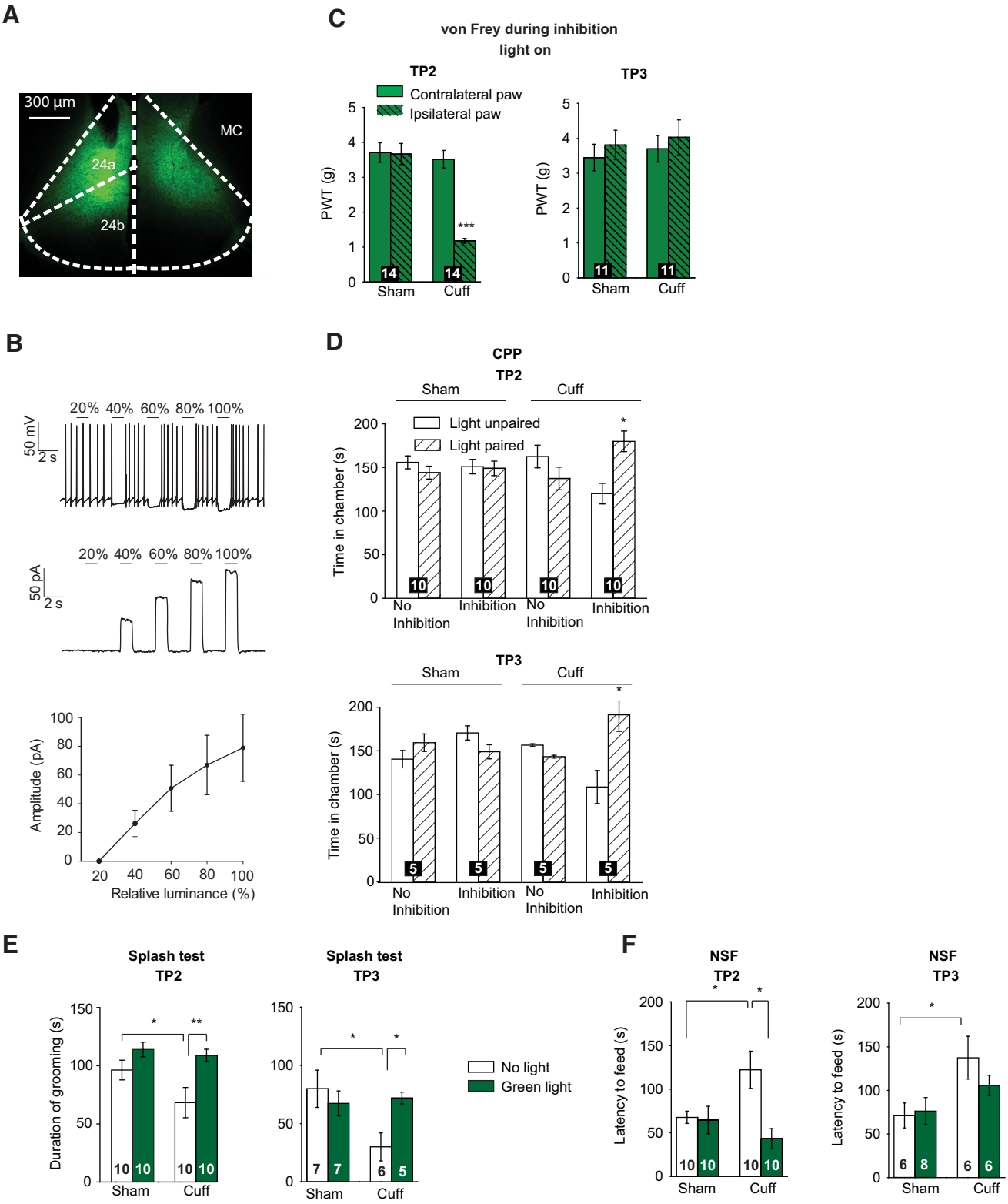

Figure 7. Optogenetic ACC inhibition blocks the aversiveness of ongoing pain and the anxiodepressive-like consequences of neuropathic pain. ***A***, Representative picture of an AAV5-CaMKII-eArchT3.0-EYFP site 5 weeks after transfection. ***B***, Light-evoked effects recorded in the ACC pyramidal neurons of AAV5-CaMKIIa-eArchT3.0-EYFP-injected mice. Top, Representative trace recorded in the current-clamp mode (note the full inhibition of spikes at all tested luminances). Middle, Representative trace of light-evoked currents recorded in the voltage-clamp mode. Bottom, Luminance-response curve of light-evoked currents ($n = 6$). The maximal luminance corresponds to 16 mW. ***C***, Mechanical hypersensitivity is not affected by ACC inhibition at both TP2 and TP3. PWT, Paw withdrawal threshold. ***D***, Optogenetic inhibition of the ACC induces a place preference at TP2 and TP3 in nerve-injured animals (but not in Sham animals) for the chamber in which light was delivered. ***E***, ACC optogenetic inhibition during the splash test reverses the decreased grooming behavior observed in nerve-injured nonstimulated animals at both TP2 and TP3. ***F***, ACC optogenetic inhibition 5 min before NSF test blocks the cuff-induced increased latency to feed at TP2. TP2 corresponds to animals displaying both mechanical hypersensitivity and anxiodepressive-like consequences. TP3 corresponds to animals that recovered from mechanical hypersensitivity but still displayed depressive-like consequences. For the CPP, Splash, and NSF experiments, the laser stimulation used was continuous green light (520 nm) for 5 min at 16 mW. Data are mean ± SEM. Numbers in the bars indicate the number of animals. *$p < 0.05$, **$p < 0.01$, ***$p < 0.001$. MC, Motor cortex.

(Benison et al., 2011; Barthas et al., 2015) without affecting ongoing pain (Barthas et al., 2015). In addition, large-diameter fibers of the dorsal column were proposed to mediate mechanical hypersensitivity but not ongoing pain (King et al., 2011). This dichotomy should thus be taken into consideration for drug development because mechanical hypersensitivity, rather than ongoing pain, is presently used for target validation. As it is more often ongoing pain that leads patients to seek treatment, this may in part explain why the development of new treatments has not always provided translational satisfaction.

While mechanical hypersensitivity is no longer present ~3 months after operation, we still observed depressive-like behaviors. Previously, it has been reported in mice that anxiodepressive-like behaviors can persist at least 10 d after normalization of mechanical sensitivity following cuff removal (Dimitrov et al., 2014). Our results confirm and further extend this hypersensitivity/affective dichotomy by showing that aversiveness and depressive-like symptoms persist at least 3–6 weeks after cessation of hypersensitivity. We also show that recovery from anxiety-like behaviors is faster, happening almost 6 weeks before the loss of depressive-like consequences, and that it coincides with the disappearance of mechanical hypersensitivity. It is important to consider that the detailed time courses for the various behavioral consequences of neuropathic pain likely depend on the considered species, strain, and pain model or etiology, as already suggested by published reports (Yalcin et al., 2014a).

The prolonged emotional consequences point out the presence of long-term plastic changes in the brain, secondary to a peripheral nerve injury. One of the cortical regions where such morphological (Blom et al., 2014; Yalcin et al., 2014b), molecular (Barthas et al., 2017), and functional plasticity (Li et al., 2010; Koga et al., 2015) has been reported is the ACC. Our *in vivo* single-unit extracellular recordings showed an increased firing rate and bursting activity in the ACC at TP2 and TP3, coinciding with aversive and depressive-like behaviors. Interestingly, the ACC hyperactivity persists even after anxiety-like behaviors disappeared, suggesting that this hyperactivity may be important but not sufficient for the anxiety-like behavior. In humans, fMRI studies have shown that the ventral part of the ACC, which is involved in emotional processing (Kanske and Kotz, 2012), is hyperactive in depressed patients (Mayberg et al., 1999; Yoshimura et al., 2010), and that activity patterns in ACC subregions correlated with symptom clusters, such as sadness and depressed mood (Mayberg et al., 1999). This possible role of ACC is further supported by animal studies showing increased cingulate cortex activity accompanying depressive-like behaviors in a social-defeat paradigm, as evidenced by c-Fos overexpression (Yu et al., 2011), and in the present model of nerve-injured mice, as evidenced by enhanced phosphorylation of the transcription factors cAMP response element binding protein and activating transcription factor as well as by enhanced cAMP responsive element-driven transcriptional activity and by c-Fos expression (Barthas et al., 2017). While it has been hypothesized that the abnormal ACC activity in depression can be associated with changes in GABA interneurons because levels of somatostatin (Seney et al., 2015) and parvalbumin (Tripp et al., 2012) are low in patients with major depressive disorders (Northoff and Sibille, 2014), 80% of ACC neurons are pyramidal ones, and the optogenetic inhibition of CaMKII-expressing ACC neurons blocks the anxiodepressive-like behaviors induced by chronic pain. Moreover, we previously showed that optogenetic activation of pyramidal neurons was sufficient to drive anxiodepressive-like behaviors in naive mice (Barthas et al., 2015, 2017). While these data indirectly support an implication of pyramidal neurons in ACC hyperactivity, the shape of spikes did not allow differentiating neuronal subtypes responsible for the *in vivo* increased firing activity. However, our *ex vivo* recordings further show that ACC might also be linked to a long-term increase in excitatory synaptic transmission. This hyperactivity could be supported by long-term alterations in functional connections onto pyramidal neurons, which may be initiated at an early stage of the neuropathy (Koga et al., 2015) and participate in the long-lasting presence of affective symptoms. Here, all the recordings were performed in layers II-III because these neurons receive both sensory inputs from the thalamus and inputs from the basal forebrain, including amygdala ones; and we previously reported that synapses in layers II-III undergo plastic changes after LTP induction or peripheral nerve injury (Koga et al., 2015; Song et al., 2017).

To leap from correlative analyses to a causal link between ACC hyperactivity and the behavioral outputs of neuropathic pain, we performed optogenetic inhibition of the ACC. We showed that the inhibition of the ACC suppressed the aversiveness of ongoing pain and the depressive-like consequences of neuropathic pain without affecting mechanical hypersensitivity at TP2 and TP3. These results further reinforce the links between pain aversiveness and depressive-like consequences on the one hand, and between ACC hyperactivity and these emotional aspects of chronic pain on the other. Together with our recent data showing that optogenetic recapitulation of the ACC hyperactivity by using channelrhodopsin 2 (Barthas et al., 2015, 2017) is sufficient to drive anxiodepressive-like behaviors in naive animals, the present data with archaerhodopsin further support the hypothesis that ACC hyperactivity is critical to anxiodepressive-like behaviors. Conversely, it has been shown that inhibiting ACC pyramidal neurons (Kang et al., 2015) or activating inhibitory neurons (Gu et al., 2015) can acutely reduce the hypersensitivity induced by Freund's complete adjuvant or formalin respectively, as also observed with pharmacological manipulation at early stages of neuropathic pain (Li et al., 2010). It suggests that ACC manipulation might also affect nociceptive hypersensitivity in given conditions.

In conclusion, our results emphasize that anxiodepressive-like consequences of chronic pain can experimentally be segregated from mechanical hypersensitivity in a time-dependent manner, whereas they follow the same time course as the aversiveness of ongoing pain. This time dependency between symptoms should be taken into consideration to improve the translational features of preclinical models, and for preclinical target validation of relevant potential therapies. The fact that the emotional consequences of chronic pain are driven by ACC hyperactivity further highlights the ACC and its circuitry as critical neuroanatomical substrates to further explore mood disorder mechanisms. Such circuitry analysis requires a precise knowledge of the ACC connectome, which was recently detailed in mice (Fillinger et al., 2017a, b). Together with present behavioral characterization and electrophysiological data, this information should now allow reaching circuit-level of analysis, including concerning the question of critical input(s) required to induce ACC hyperactivity, and of whether maintaining ACC hyperactivity requires or not input(s) hyperactivity.

Note Added in Proof: The 12th author was left out of the author line in the early release version of this article that was published online on February 20, 2018. The author line has since been corrected.

References

Alba-Delgado C, Llorca-Torralba M, Horrillo I, Ortega JE, Mico JA, Sánchez-Blázquez P, Meana JJ, Berrocoso E (2013) Chronic pain leads to con-

comitant noradrenergic impairment and mood disorders. Biol Psychiatry 73:54–62. CrossRef Medline

Barrot M (2012) Tests and models of nociception and pain in rodents. Neuroscience 211:39–50. CrossRef Medline

Barthas F, Sellmeijer J, Hugel S, Waltisperger E, Barrot M, Yalcin I (2015) The anterior cingulate cortex is a critical hub for pain-induced depression. Biol Psychiatry 77:236–245. CrossRef Medline

Barthas F, Humo M, Gilsbach R, Waltisperger E, Karatas M, Leman S, Hein L, Belzung C, Boutillier AL, Barrot M, Yalcin I (2017) Cingulate overexpression of mitogen-activated protein kinase phosphatase-1 as a key factor for depression. Biol Psychiatry 82:370–379. CrossRef Medline

Benbouzid M, Choucair-Jaafar N, Yalcin I, Waltisperger E, Muller A, Freund-Mercier MJ, Barrot M (2008) Chronic, but not acute, tricyclic antidepressant treatment alleviates neuropathic allodynia after sciatic nerve cuffing in mice. Eur J Pain 12:1008–1017. CrossRef Medline

Benison AM, Chumachenko S, Harrison JA, Maier SF, Falci SP, Watkins LR, Barth DS (2011) Caudal granular insular cortex is sufficient and necessary for the long-term maintenance of allodynic behavior in the rat attributable to mononeuropathy. J Neurosci 31:6317–6328. CrossRef Medline

Bliss TV, Collingridge GL, Kaang BK, Zhuo M (2016) Synaptic plasticity in the anterior cingulate cortex in acute and chronic pain. Nat Rev Neurosci 17:485–496. CrossRef Medline

Blom SM, Pfister JP, Santello M, Senn weeks, Nevian T (2014) Nerve injury-induced neuropathic pain causes disinhibition of the anterior cingulate cortex. J Neurosci 34:5754–5764. CrossRef Medline

Chen T, Koga K, Descalzi G, Qiu S, Wang J, Zhang LS, Zhang ZJ, He XB, Qin X, Xu FQ, Hu J, Wei F, Huganir RL, Li YQ, Zhuo M (2014) Postsynaptic potentiation of corticospinal projecting neurons in the anterior cingulate cortex after nerve injury. Mol Pain 10:33. CrossRef Medline

Cordeiro Matos S, Zhang Z, Séguéla P (2015) Peripheral neuropathy induces HCN channel dysfunction in pyramidal neurons of the medial prefrontal cortex. J Neurosci 35:13244–13256. CrossRef Medline

Dimitrov EL, Tsuda MC, Cameron HA, Usdin TB (2014) Anxiety- and depression-like behavior and impaired neurogenesis evoked by peripheral neuropathy persist following resolution of prolonged tactile hypersensitivity. J Neurosci 34:12304–12312. CrossRef Medline

Drevets WC, Bogers weeks, Raichle ME (2002) Functional anatomical correlates of antidepressant drug treatment assessed using PET measures of regional glucose metabolism. Eur Neuropsychopharmacol 12:527–544. CrossRef Medline

Fillinger C, Yalcin I, Barrot M, Veinante P (2017a) Efferents of anterior cingulate areas 24a and 24b and midcingulate areas 24a′ and 24b′ in the mouse. Brain Struct Funct. Advance online publication. Retrieved Dec. 6, 2017. doi: 10.1007/s00429–017-1585-x. CrossRef Medline

Fillinger C, Yalcin I, Barrot M, Veinante P (2017b) Afferents to anterior cingulate areas 24a and 24b and midcingulate areas 24a′ and 24b′ in the mouse. Brain Struct Funct 222:1509–1532. CrossRef Medline

Gonçalves L, Silva R, Pinto-Ribeiro F, Pêgo JM, Bessa JM, Pertovaara A, Sousa N, Almeida A (2008) Neuropathic pain is associated with depressive behaviour and induces neuroplasticity in the amygdala of the rat. Exp Neurol 213:48–56. CrossRef Medline

Gu L, Uhelski ML, Anand S, Romero-Ortega M, Kim YT, Fuchs PN, Mohanty SK (2015) Pain inhibition by optogenetic activation of specific anterior cingulate cortical neurons. PLoS One 10:e0117746. CrossRef Medline

Johansen JP, Fields HL, Manning BH (2001) The affective component of pain in rodents: direct evidence for a contribution of the anterior cingulate cortex. Proc Natl Acad Sci U S A 98:8077–8082. CrossRef Medline

Kang SJ, Kwak C, Lee J, Sim SE, Shim J, Choi T, Collingridge GL, Zhuo M, Kaang BK (2015) Bidirectional modulation of hyperalgesia via the specific control of excitatory and inhibitory neuronal activity in the ACC. Mol Brain 8:81. CrossRef Medline

Kanske P, Kotz SA (2012) Effortful control, depression, and anxiety correlate with the influence of emotion on executive attentional control. Biol Psychol 91:88–95. CrossRef Medline

King T, Vera-Portocarrero L, Gutierrez T, Vanderah TW, Dussor G, Lai J, Fields HL, Porreca F (2009) Unmasking the tonic-aversive state in neuropathic pain. Nat Neurosci 12:1364–1366. CrossRef Medline

King T, Qu C, Okun A, Mercado R, Ren J, Brion T, Lai J, Porreca F (2011) Contribution of afferent pathways to nerve injury-induced spontaneous pain and evoked hypersensitivity. Pain 152:1997–2005. CrossRef Medline

Koga K, Descalzi G, Chen T, Ko HG, Lu J, Li S, Son J, Kim T, Kwak C, Huganir RL, Zhao MG, Kaang BK, Collingridge GL, Zhuo M (2015) Coexistence of two forms of LTP in ACC provides a synaptic mechanism for the interactions between anxiety and chronic pain. Neuron 85:377–389. CrossRef Medline

Li XY, Ko HG, Chen T, Descalzi G, Koga K, Wang H, Kim SS, Shang Y, Kwak C, Park SW, Shim J, Lee K, Collingridge GL, Kaang BK, Zhuo M (2010) Alleviating neuropathic pain hypersensitivity by inhibiting PKMzeta in the anterior cingulate cortex. Science 330:1400–1404. CrossRef Medline

Mayberg HS, Liotti M, Brannan SK, McGinnis S, Mahurin RK, Jerabek PA, Silva JA, Tekell JL, Martin CC, Lancaster JL, Fox PT (1999) Reciprocal limbic-cortical function and negative mood: converging PET findings in depression and normal sadness. Am J Psychiatry 156:675–682. CrossRef Medline

Narita M, Kaneko C, Miyoshi K, Nagumo Y, Kuzumaki N, Nakajima M, Nanjo K, Matsuzawa K, Yamazaki M, Suzuki T (2006) Chronic pain induces anxiety with concomitant changes in opioidergic function in the amygdala. Neuropsychopharmacology 31:739–750. CrossRef Medline

Northoff G, Sibille E (2014) Why are cortical GABA neurons relevant to internal focus in depression[quest] A cross-level model linking cellular, biochemical and neural network findings. Mol Psychiatry 19:966–977. CrossRef Medline

Peyron R, García-Larrea L, Grégoire MC, Convers P, Richard A, Lavenne F, Barral FG, Mauguière F, Michel D, Laurent B (2000) Parietal and cingulate processes in central pain: a combined positron emission tomography (PET) and functional magnetic resonance imaging (fMRI) study of an unusual case. Pain 84:77–87. CrossRef Medline

Porsolt RD, Le Pichon M, Jalfre M (1977) Depression: a new animal model sensitive to antidepressant treatments. Nature 266:730–732. CrossRef Medline

Qu C, King T, Okun A, Lai J, Fields HL, Porreca F (2011) Lesion of the rostral anterior cingulate cortex eliminates the aversiveness of spontaneous neuropathic pain following partial or complete axotomy. Pain 152:1641–1648. CrossRef Medline

Radat F, Margot-Duclot A, Attal N (2013) Psychiatric co-morbidities in patients with chronic peripheral neuropathic pain: a multicentre cohort study. Eur J Pain 17:1547–1557. CrossRef Medline

Sellmeijer J (2016) Analysis electrophys. Available at https://bitbucket.org/jsellmeijer/analysis_electrophys/commits/7c2d9026c770c42211c2fd34b44328dbc25b4666?at=master

Seney ML, Tripp A, McCune S, Lewis DA, Sibille E (2015) Laminar and cellular analyses of reduced somatostatin gene expression in the subgenual anterior cingulate cortex in major depression. Neurobiol Dis 73:213–219. CrossRef Medline

Shackman AJ, Salomons TV, Slagter HA, Fox AS, Winter JJ, Davidson RJ (2011) The integration of negative affect, pain and cognitive control in the cingulate cortex. Nat Rev Neurosci 12:154–167. CrossRef Medline

Song Q, Zheng HW, Li XH, Huganir RL, Kuner T, Zhuo M, Chen T (2017) Selective phosphorylation of AMPA receptor contributes to the network of long-term potentiation in the anterior cingulate cortex. J Neurosci 37:8534–8548. Medline

Surget A, Wang Y, Leman S, Ibarguen-Vargas Y, Edgar N, Griebel G, Belzung C, Sibille E (2009) Corticolimbic transcriptome changes are state-dependent and region-specific in a rodent model of depression and of antidepressant reversal. Neuropsychopharmacology 34:1363–1380. CrossRef Medline

Suzuki T, Amata M, Sakaue G, Nishimura S, Inoue T, Shibata M, Mashimo T (2007) Experimental neuropathy in mice is associated with delayed behavioral changes related to anxiety and depression. Anesth Analg 104:1570–1577. CrossRef Medline

Tang J, Ko S, Ding HK, Qiu CS, Calejesan AA, Zhuo M (2005) Pavlovian fear memory induced by activation in the anterior cingulate cortex. Mol Pain 1:6. CrossRef Medline

Tripp A, Oh H, Guilloux JP, Martinowich K, Lewis DA, Sibille E (2012) Brain-derived neurotrophic factor signaling and subgenual anterior cingulate cortex dysfunction in major depressive disorder. Am J Psychiatry 169:1194–1202. CrossRef Medline

Vogt MA, Mallien AS, Pfeiffer N, Inta I, Gass P, Inta D (2016) Minocycline

does not evoke anxiolytic and antidepressant-like effects in C57BL/6 mice. Behav Brain Res 301:96–101. CrossRef Medline

Wang R, King T, De Felice M, Guo weeks, Ossipov MH, Porreca F (2013) Descending facilitation maintains long-term spontaneous neuropathic pain. J Pain 14:845–853. CrossRef Medline

Xu H, Wu LJ, Wang H, Zhang X, Vadakkan KI, Kim SS, Steenland HW, Zhuo M (2008) Presynaptic and postsynaptic amplifications of neuropathic pain in the anterior cingulate cortex. J Neurosci 28:7445–7453. CrossRef Medline

Yalcin I, Bohren Y, Waltisperger E, Sage-Ciocca D, Yin JC, Freund-Mercier MJ, Barrot M (2011) A time-dependent history of mood disorders in a murine model of neuropathic pain. Biol Psychiatry 70:946–953. CrossRef Medline

Yalcin I, Barthas F, Barrot M (2014a) Emotional consequences of neuropathic pain: insight from preclinical studies. Neurosci Biobehav Rev 47:154–164. CrossRef Medline

Yalcin I, Megat S, Barthas F, Waltisperger E, Kremer M, Salvat E, Barrot M (2014b) The sciatic nerve cuffing model of neuropathic pain in mice. J Vis Exp 16:89. CrossRef Medline

Yang Q, Wu Z, Hadden JK, Odem MA, Zuo Y, Crook RJ, Frost JA, Walters ET (2014) Persistent pain after spinal cord injury is maintained by primary afferent activity. J Neurosci 34:10765–10769. CrossRef Medline

Yoshimura S, Okamoto Y, Onoda K, Matsunaga M, Ueda K, Suzuki S, Shigetoyamawaki (2010) Rostral anterior cingulate cortex activity mediates the relationship between the depressive symptoms and the medial prefrontal cortex activity. J Affect Disord 122:76–85. CrossRef Medline

Yu T, Guo M, Garza J, Rendon S, Sun XL, Zhang weeks, Lu XY (2011) Cognitive and neural correlates of depression-like behaviour in socially defeated mice: an animal model of depression with cognitive dysfunction. Int J Neuropsychopharmacol 14:303–317. CrossRef Medline